Experimental studies of using wireless energy transmission for powering embedded sensor nodes

David L. Mascarenas [a], Eric B. Flynn [a], Michael D. Todd [a], Timothy G. Overly [b], Kevin M. Farinholt [b], Gyuhae Park [b,*], Charles R. Farrar [b]

[a] Department of Structural Engineering, University of California, San Diego, La Jolla, CA 92093, USA
[b] The Engineering Institute, Los Alamos National Laboratory, Mail Stop T001, Los Alamos, NM 87545, USA

ARTICLE INFO

ABSTRACT

A major challenge impeding the deployment of wireless sensor networks for structural health monitoring (SHM) is developing a means to supply power to the sensor nodes in an efficient manner. In this paper, we explore possible solutions to this challenge by using a mobile-host based wireless energy transmission system to provide both power and data interrogation commands to sensor nodes. The mobile host features the capability of wirelessly transmitting energy to sensor nodes on an as-needed basis. In addition, it serves as a central data repository and processing center for the data collected from the sensing network. The wirelessly transmitted microwave energy is captured by a receiving antenna, transformed into DC power by a rectifying circuit, and stored in a storage medium to provide the required energy to the sensor node. The application of wireless energy transmission is targeted toward SHM sensor nodes that have been recently developed by the authors, which can be used to collect peak mechanical displacements or piezoelectric impedance measurements. This paper will describe considerations needed to design such energy transmission systems, experimental procedure and results, method of increasing the efficiency, energy conditioning circuits and storage medium, and target applications. Experimental results from a field test on the Alamosa Canyon Bridge in southern New Mexico will also be presented.

Published by Elsevier Ltd.

1. Introduction

This paper describes the experimental investigation of wireless radio frequency (RF) energy transmission systems for structural health monitoring (SHM) applications. A major concern for all wireless sensor networks is the available energy supply. The conventional power supply for wireless sensor nodes is generally some form of battery. As sensor networks become more widespread and involve more active elements, the battery power supply quickly becomes unsuitable from both an operational and maintenance standpoint. The ideal solution would be to design sensor nodes with a power supply that does not need replacement over the entire projected lifetime of the sensor network. A number of different approaches have been studied in an attempt to obtain this ideal. A possible solution to the problem of localized power generation is technologies that enable harvesting ambient energy—whether thermal, vibration, acoustic, or solar—to power the instrumentation. Although extensive research work has been focused in energy harvesting, either the amount of harvested energy appears to fall significantly short of the level required by SHM sensing systems (a conversion efficiency issue) or the

---

* Corresponding author. Tel.: +1 505 663 5335.
  E-mail address: gpark@lanl.gov (G. Park).

structure simply does not have the direct ambient energy sources available. Therefore, methods of increasing the amount of energy generated by the energy harvesting device or developing new and innovative methods of accumulating the energy are the key technologies that will allow energy harvesting to become a practical source of power for wireless SHM systems [1].

An alternative power supply scheme that is being investigated by the authors is RF wireless energy transmission. Recently, the authors have proposed a new SHM sensing network paradigm [2,3], which involves using an unmanned mobile host node (delivered via unmanned aerial/ground vehicles (UV)) to generate an RF signal near a receiving antenna connected to embedded sensors on the structure. The sensors measure the desired responses at critical areas on the structure and transmit the signal back to the mobile host again via the RF communications. This wireless communications capability draws power from the RF energy transmitted between the mobile host and sensor node and uses it to both power the sensing circuit and to transmit the signal back to the host. This research takes traditional sensing networks to the next level, as the mobile hosts will travel either on the ground or in the air to the vicinity of receiving antennas connected to sensor nodes embedded in critical infrastructure, deliver required power, and then begin to perform an inspection without human intervention. The mobile hosts will move close to the receiving antennas and their associated sensors on the structure and gather critical data needed to perform the structural health evaluation. Sensors and sensor nodes could be fully embedded into a structure, as only the receiving antenna needs to be assessable by the mobile host. This integrated technology will be directly applicable to rapid structural condition assessment of buildings and bridges after a natural or man-made disaster, for example, earthquakes of ship impact on bridge piers. In addition, this approach to powering embedded sensors is particularly well suited for applications where human inspection protocols pose health or life-safety risks (e.g. inspection in a nuclear power plant structure after a damage event). Also, this technology may be adapted and applied to damage detection strategies in a variety of engineering systems.

The wireless energy transmission technology that has received the most attention in the last 50 years is that of microwave transmission. Originally considered as a concept for use with space-based solar power satellites, it has been significantly improved in the last several decades. Microwaves are transmitted across the atmosphere or space to a receiver, which can either be a typical antenna (with rectifying circuitry to return the microwaves to DC power) or a rectenna (rectifying-antenna) which integrates the technology to receive and directly convert the microwaves into DC power. This design typically allows for much higher efficiencies. A pair of excellent survey articles was written to discuss the history of microwave power [4,5]. With the use of rectennas, efficiencies in the 50–80 percent range of DC to DC conversion have been achieved. Significant testing of microwave energy delivery has also been done across long distances and with kW power levels [6]. Their study showed the feasibility of the energy delivery systems for actuating large devices, including DC motors and high-power piezoelectric actuators. However the application of this technology to low-power electronics has not been substantially studied outside of RFID applications. In particular, the application of wireless power transmission for SHM sensor nodes in order to alleviate the challenges associated with power supply issues has never been addressed in the literature. Therefore, in this study, we experimentally investigate the RF wireless energy transmission as an alternative power source for wireless SHM sensor nodes.

The following discussion will cover the theory behind wireless energy transmission, the hardware developed to implement wireless energy transmission, as well as experimental results in the lab and from a field test at the Alamosa Canyon Bridge in August 2007. In this test, the RF energy transmission equipment was attached to a radio control (RC) helicopter or a human-controlled vehicle.

2. Theoretical overview of wireless energy transmission

An outline of the theory used to describe wireless energy transmission by electromagnetic waves is given in [7]. A short description will be given here. In this work, RF energy was typically transmitted at 2.5 GHz. This band was chosen as the transmission frequency for a variety of reasons including the ease of obtaining commercially available hardware and the ability to buy high-gain antennas with a weight and volume appropriate for a mobile host. The Friis formula can be used to describe the RF energy transmission:

$$P_R = \frac{G_T G_R \lambda^2}{(4\pi R)^2} P_T \tag{1}$$

In this equation P_R is the power received, G_T is the gain of the transmitter antenna, G_R is the gain of the receiver antenna, λ is the wavelength of the radiation, R is the distance, and P_T is the power transmitted. The wavelength is given by

$$\lambda = \frac{c}{f} \tag{2}$$

In this expression c is the speed of light, and f is the frequency of the single-tone signal. The typical Friis-link parameters used in the following theoretical investigation are shown in Fig. 1. In Fig. 1, the gain (dB) is defined as

$$Gain \ (\text{dB}) = 10 \times \text{Log}_{10}(Gain(linearscale)) \tag{3}$$

The transmission (Tx) antenna is a 14.5 dBi Yagi antenna, and the receiver (Rx) antenna is a 19 dBi patch antenna. Two meters was selected as an estimated distance based on a reasonable limit of proximity that the mobile host could be able to
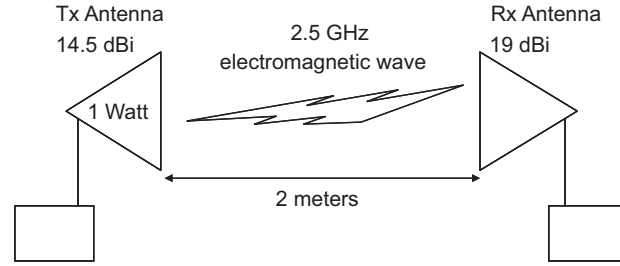
Fig. 1. Typical wireless energy transmission parameters and test setup used in this investigation.

approach the sensor node. The values in Fig. 1 can be used with Eqs. (1) and (2) to estimate the theoretical power transmission to the sensor node, assuming 100 percent efficiency.

$$\lambda = \frac{c}{f} = \frac{3 \times 10^8 \, \text{m/s}}{2.5 \times 10^9 \, \text{Hz}} = 0.12 \, \text{m} \tag{4}$$

$$P_R = \frac{(28.18)(79.43)(0.12 \, \text{m})^2}{(4\pi(2 \, \text{m}))^2} 1 \, \text{W} = 0.051 \, \text{W} \tag{5}$$

The maximum amount of power, P_R, which can be theoretically received at the Rx antenna is 51 mW. In Eq. (5), the gain values in dB, G_T (14.5 dB) and G_R (19 dB), are converted to 28.18 and 79.43, respectively with the Eq. (3). When the power is received at the antenna, it then passes through the rectification circuitry to supply a DC voltage to charge an energy storage medium, such as a supercapacitor. If one uses a 0.1 F super capacitor and charges it up to 3.5 V, the lowest possible time to charge the capacitor can be calculated. Eq. (5) gives the expression for calculating the energy in a capacitor.

$$E = \tfrac{1}{2}CV^2 \tag{6}$$

In this expression, E is the energy, C is the capacitance, and V is the voltage. Inserting the relevant information yields

$$E = \tfrac{1}{2}(0.1 \, \text{F})(3.5 \, \text{V})^2 = 0.6125 \, \text{J} \tag{7}$$

$$Time = \frac{E}{P_R} = \frac{0.6125 \, \text{J}}{0.051 \, \text{W}} = 12.0 \, \text{s} \tag{8}$$

So for the assumed 2 m distance, the capacitor can be charged in no less than 12 s assuming there are no losses due to the rectifier, antennas, destructive interference, misalignment errors and positioning errors.

3. RF energy transmission implementation overview

An overview of the wireless energy transmission system implementation is shown in Fig. 2. An array of sensors and sensor nodes are deployed on a structure. If the data are needed for structural health evaluation, a mobile-host can be sent to these sensor nodes on the structure. The mobile-host is equipped with an RF generator and computational payload that allows the "mobile-host" to wirelessly transmit energy to a given sensor node in order to provide power. The mobile host also features an on-board computer with a Zigbee radio and 802.11 g wireless card for receiving data transmitted by the base station and sensor node. The computer is meant to be able to collect data from the sensor node and store it for future use. In a wide-scale sensor network, the helicopter would fly throughout the sensor network and collect data from every sensor of interest. The helicopter would serve as a central data repository and central data processing node for the sensor network. The mobile-host deployed in this application is a Spectra-G radio-controlled helicopter from Miniature Aircraft USA, shown in the middle of Fig. 2, which has a rotor diameter of 1.6 m. This work will focus on the first implementation of the "roving-host" wireless sensor network.

4. Components of RF energy transmission systems

Several hardware and software components were designed and implemented for this proposed sensing network. These components are RF/computational payload, a mobile-host (helicopter), Rx and Tx antennas, a RF to DC converter, 0.1 F super capacitors, a voltage threshold switch, sensors, and sensor nodes. A slightly modified system that uses a ground vehicle as a mobile host is also briefly described in this section.
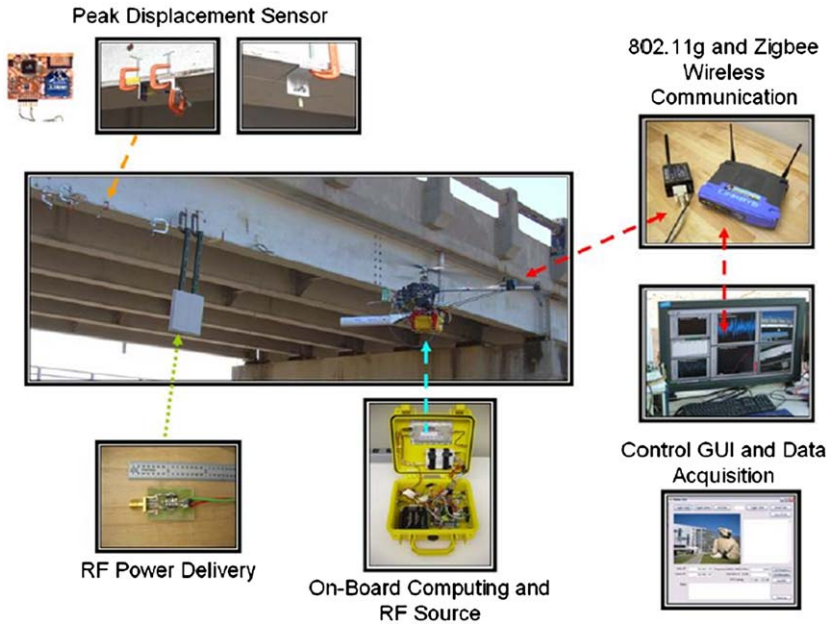
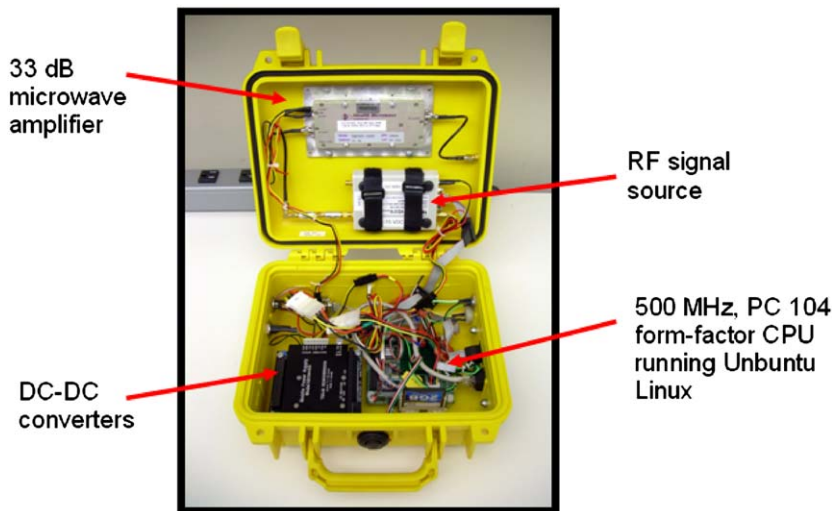**Fig. 2.** Summary of components used for the "roving host" wireless sensor network.

Fig. 3. RF and computational payload carried by the "mobile host".

4.1. RF/computational payload

The computing source on the helicopter is provided by an AMD Geode LX 800 CPU running Unbuntu Linux. The computer boots from a compact-flash card for weight savings and to eliminate moving parts within the helicopter payload that might compromise reliability. This computer controls a NovaSource RF signal generator via an RS-232 connection. The RF source sends signals to the RF amplifier so the power level is suitably high for wireless power transmission ($\sim$1 W). The computer is running Apache web server, allowing command and control of the computer and RF source from the base station via 802.11 g wireless network. Data are received from the sensor node via an RS-232 enabled XBee modem (manufactured by XStream). The data are stored in the helicopter memory until requested by the base station. Fig. 3 shows the helicopter on-board computing package. The RF/computational payload is powered by two separate lithium-polymer batteries.

4.2. Mobile host (X-Cell Spectra G Helicopter)

The helicopter airframe used in this test is the X-Cell Spectra G. The helicopter power plant is a 23 cc, two-cycle gas engine. The helicopter is using 810 mm anti-symmetrical, high-lift blades to carry the computational and RF payload. In addition, the stock exhaust was exchanged for a Hatori muffler, enabling a broadened power curve. The helicopter weighs approximately 5.4 kg ready to fly in the stock condition. When loaded with the sensor network payload, the total weight of the helicopter rose close to 10 kg. The helicopter is also carrying an Axis 207 W wireless webcam for recording events as seen by the helicopter. Fig. 4 shows the various components on the helicopter.

4.3. Transmitting antenna

The mobile-host transmits a 2.5 GHz signal through a 14.5 dBi Yagi antenna, as shown in Fig. 5. The antenna is basically cylindrical in shape due to the radome covering the actual Yagi antenna itself. The overall dimensions of the antenna are 476 mm × 76.2 mm diameter. There are several factors to consider when selecting an antenna for the helicopter, including weight, size, ease of mounting, and gain. The antenna should be light-weight and small in size and should not adversely
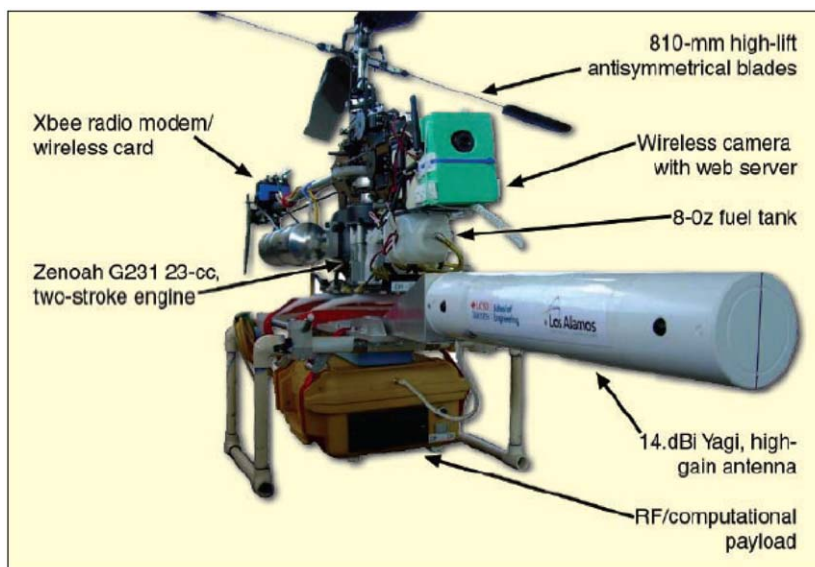

Fig. 4. The mobile-host helicopter and its component.

Fig. 5. Yagi antenna used to transmit RF energy.

affect the balance of the helicopter. Furthermore, the antenna should have relatively high gain for a higher power transfer, but not so high gain that the pointing accuracy of the helicopter would have to be excessively accurate. As in Eq. (1), the higher the gain of the antennas, the higher is the energy transmission to the receiver. However as gain increases, the main lobe of the antenna decreases in size, thus requiring more precise alignment between the receiving and the transmitting antenna. For a description of how changes in gain affect beamwidth for antenna with a single main lobe and negligible minor lobes similar to a Yagi–Uda antenna, please refer Ref. [8]. Another concern with high-gain antennas is that as antennas increase in gain, they also increase in size and weight. The characteristic size of the antenna depends on the wavelength of the radiation being transmitted from it. This is a major reason why 2.5 GHz with a wavelength of 0.120 m was chosen as the RF signal frequency over other widely used frequencies such as 900 MHz with a wavelength of 0.333 m. Antennas of 900 MHz with comparable gain were deemed too large for the initial test of the mobile-host wireless sensor network. The Yagi antenna was chosen because of its high-gain, light-weight, and acceptable cost. The shape and size of the Yagi is conducive to being placed in the front of the helicopter and easy to mount.

4.4. Receiving antenna

The receiving antenna selected for this investigation is shown in Fig. 6. The antenna shown is a 19 dBi patch antenna with overall dimensions of $387 \times 387 \times 25$ mm. The main driving factors for the selection of the receiving antenna were overall size and gain. Another important consideration was the wind loading when the antenna is installed in a structure. The chosen antenna should not have a size and shape that would facilitate high wind loading, or snow loading. If the antenna could experience these types of loads, there was concern that the antenna might be difficult to align with the helicopter on a windy day due to vibration. Under severe wind loading, the antenna might even break off the structure. For these reasons, the receiver antenna should have a low profile. Weight was not as large a factor because the antenna would be placed on a structure. The esthetic nature of the antenna was also of concern because, in some applications, it may be mounted within view of the public. The antenna should also facilitate alignment with the transmitting antenna on the helicopter. A patch antenna was selected because of its low profile on the bridge and the ease of mounting and alignment with the helicopter. Furthermore, of all the antennas considered, the patch antenna had the highest gain.

Concern also has to be taken when mounting the antenna on the structure. Civil structures such as buildings and bridges often contain structural elements which can facilitate multipath distortion. Multipath distortion is caused when signals take more than a single path to travel between two locations. In general, the time the signal takes to travel along different paths is different from path to path. The effective result is that multiple identical signals arrive at the final location out of phase. The effect on RF energy transmission applications of the out of phase arrivals is that nulls and peaks are created in the spatial electromagnetic field. There may be some locations where the efficiency of RF energy transmission is either greatly reduced or improved. In general, multipath distortion is an undesirable phenomenon. Structural elements which can give rise to multipath distortion include steel girders, metal siding, metal-coated glass, ground vehicles, metal guard rails, etc. Multipath distortion effects should be considered when selecting a mounting location for the receiver antenna. Please see [9] for more discussion of the multipath distortion phenomenon.
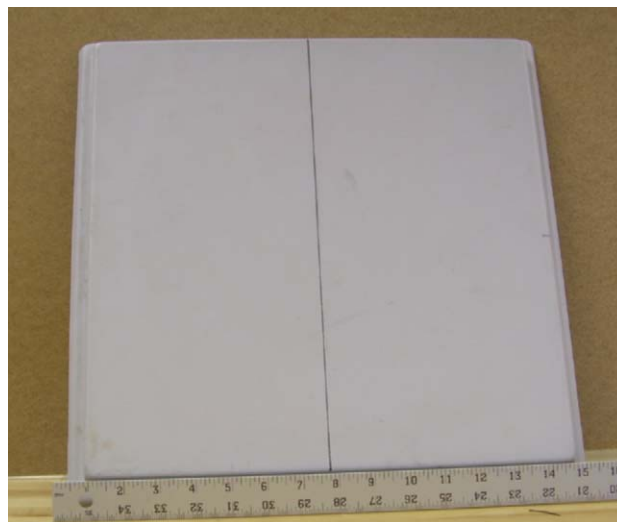

Fig. 6. 19 dBi Yagi patch antenna used for receiving wireless energy transmissions from the helicopter.
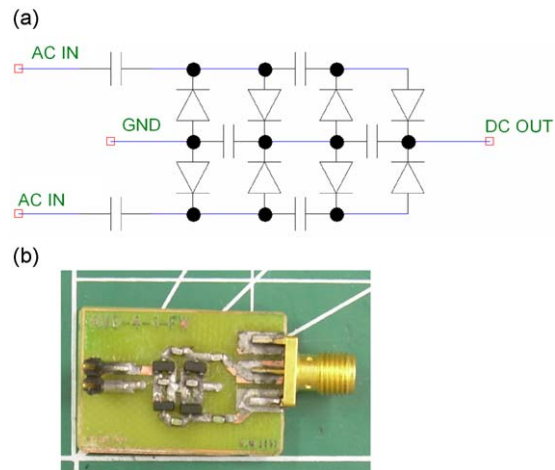
Fig. 7. Full-wave voltage quadrupler RF to DC converter. (a) Schematic view and (b) physical implementation.

4.5. RF to DC converter

A vital portion of the RF energy transmission process is converting the received RF energy to DC energy which can then be stored in a supercapacitor. The combination of a receiver antenna and an RF to DC converter is commonly referred to in the literature as a "rectenna". Please see [4] for a thorough discussion on the history of rectenna research. It is desirable that the RF to DC converter be relatively low-cost, small size, and high efficiency. Furthermore, it is vitally important that the RF to DC converter be able to supply the DC output voltage at a high level so that it can charge the capacitor to an acceptable level. In this work, a multiple-stage RF voltage multiplier or a full-wave voltage quadrupler, effectively rectifies the RF to DC and also multiplies the DC output voltage. A detailed discussion on voltage multipliers operations and design considerations is given in [10]. The schematic for the full-wave configuration is shown in Fig. 7a and the hardware implementation of the full-wave voltage quadrupler is shown in Fig. 7b. The diodes used in this application were the HSMS 8202 surface mount microwave Schottky mixer diodes. These diodes are microwave diodes designed to operate correctly on signals up to 14 GHz. It should be noted that the diodes are a major source of energy dissipation after receiving the RF energy.

After fabrication, the full-wave rectifier was tested using the parameters described in the theoretical section. Although a 51 mW of theoretical maximum power was estimated in Eq. (4), experimentally it was identified that only 8.1 mW of average power was converted due to the energy dissipation, primarily caused by the diodes. This test also showed that it took 95 s to charge the 0.1 F super capacitor.

4.6. Voltage threshold turn-on switch

Once the energy has been transmitted by the mobile host, and has been stored in the sensor node's capacitor, the next step is to deliver the energy to the electronic components on the sensor node. The problem is that, if the sensor node is directly connected to the 0.1 F supercapacitor, the node will attempt to turn on and drain the energy before enough energy is accumulated for the proper operation of the sensor node. It would therefore be absolutely necessary to develop some form of "switch" to make sure that the sensor node does not receive any energy until the capacitor is fully charged to the desired voltage. This switch has some very stringent requirements. First, it would need to have a very high impedance when the switch is in the open position so that no energy would reach the sensor node until the correct time. The switch must toggle to the closed position when the capacitor voltage had reached the desired level. The switch would have to consume power on the order of hundreds of microwatts at most. Furthermore, the switch would have to be capable of operating without any form of stored energy. To the author's best knowledge, a switch fulfilling the requirements is not currently commercially available. Furthermore, techniques such as periodic sampling of the capacitor voltage with an analog-to-digital (A/D) converter are not practical because, during a large fraction of the charging time, the voltage available from the capacitor is not high enough to run the microcontroller or the A/D converter.

To solve the problem, a switch made up of micro-power comparators utilizing voltage-band gap references, low-voltage analog switches and a high impedance voltage divider was developed. The block diagram representation of the switch is shown in Fig. 8. The operation of the voltage threshold turn-on switch can be described as follows. As the 0.1 F capacitor is charged, a very small fraction of the current is used to excite a high-impedance voltage divider connected to a comparator. The other pin of the comparator is connected to a 1.24 V band gap voltage reference. Once the voltage on the capacitor
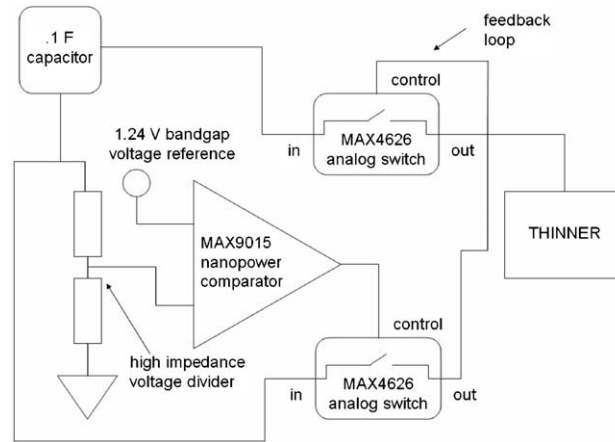
Fig. 8. Block diagram of voltage threshold turn-on switch.

reaches a value such that the output of the voltage divider exceeds the 1.24 V supplied by the voltage bandgap reference, the comparator sends a signal to a MAX4626 normally-open analog switch, thus signaling the switch to close. Once the switch closes, current from the capacitor is allowed to flow through the first switch, and then into the control pin of a second normally open switch. The second normally open switch is connected between the 0.1 F capacitor and the sensor node. At this point current begins to flow from the capacitor through the second switch and into the sensor node. In addition, current also flows from the capacitor through the switch, and through a feedback loop into the control pin of the second switch, thus ensuring that the second switch remains in the closed position throughout the complete discharge of the 0.1 F capacitor. Power for the comparators and switches is supplied by the energy in the capacitor as it is charged. The voltage on the capacitor at which the switch allows current to flow is controlled by the values of the resistors in the high-impedance voltage divider.

4.7. Sensor nodes

The wireless sensor nodes developed in this work are known as "THINNER". THINNER is intended to collect peak mechanical displacement measurements for civil infrastructure applications. The THINNER sensor node utilizes a capacitance-to-digital converter instead of a conventional voltage-based analog-to-digital (A/D) converter, which allows the sensor node directly coupled with the capacitive-based sensors. The selected converter was the AD7745 from Analog Devices. The AD7745 can measure capacitance in the range of 0 and 21 pF with ± 4 fF accuracy. In addition, the AD7745 has a temperature sensor and a conventional voltage-based A/D converter. This chip uses a voltage range of 2.7–5.25 V and consumes 700 μA of current at 3.3 V.

A peak displacement sensor capable of storing peak values in the absence of electrical energy was also developed. The sensor used in this work is very similar to that developed in [11] and utilizes essentially the same operation principle. The peak displacement sensor is essentially a parallel plate capacitor in a cylindrical configuration. The inner and outer aluminum components are the two plates of the capacitor and he capacitance of the sensor changes when the inner and outer cylinders are moved relative to one another along the axis of the cylinders.

WID2 was also designed and tested by our research team. The WID2 capitalizes on the well-established impedance-based structural health monitoring technique. The device is particularly unique because it offers a low-cost, low-power, wireless capabilities, and data processing not seen in any other impedance measurement hardware available today. The detailed description on these devices is presented in a separate article [12].

4.8. A mobile-host based on ground vehicle

A slightly modified system was also designed for a ground vehicle as a mobile host, as shown in Fig. 9. A ground vehicle mobile host would be useful for civil structures, such as bridges. The energy transmission equipment was mounted within the mobile host vehicle. The entire system was powered through the DC outlet of the vehicle, using a power inverter to provide AC power for the benchtop power supplies used for the signal generator and microwave amplifier. The NovaSource signal generator was tuned to provide a 2.45 GHz excitation signal which was fed through a microwave amplifier and supplied to the parabolic grid antenna.

A receiving patch antenna was also designed and tested. For a single microstrip patch antenna, the power efficiency is calculated to be approximately 1.2 percent at 1 m spacing [13]. Such low efficiency is attributed to the small size of the

Fig. 9. An energy transmission system based on a ground vehicle.

Fig. 10. Alamosa Canyon Bridge test setup.

individual microstrip patch antenna which measures 3.4 cm × 3.4 cm. While the individual antennas have a very low associated gain, the performance can be greatly enhanced by assembling them into large arrays. Eighteen element arrays, like the one shown in Fig. 9, can be fabricated with relative ease. This configuration greatly enhances the receiving antennas performance as the array is capable of harvesting much more of the incident wave generated by the source antenna. Additionally, the output of the antenna can be connected in a variety of configurations to tune the amount of voltage harvested from the antenna. In the orientation shown in Fig. 9, the patch antennas are connected in groups of three (each in series), with these groups subsequently connected in parallel to increase current. Laboratory tests have shown that this antenna array is capable of charging a 0.1 F capacitor to 3.3 V in 24 s, when located 1 m from a source antenna that is emitting 910 mW of microwave power at 2.45 GHz.

5. Experimental test results

5.1. RF energy transmission to the THINNER sensor node using helicopter

The first full-scale test of the mobile-host wireless sensor nodes was at the Alamosa Canyon Bridge in southern New Mexico. The THINNER sensor node was placed on the understructure of the bridge. A capacitive peak displacement sensor was connected to a THINNER. The 19 dBi receiving antenna was hung slightly below the longitudinal steel bridge supports.

The RF energy transmission equipment was placed on an RC spectra G helicopter, which was manually flown up to the 19 dBi patch antenna on the bridge to charge up the THINNER sensor node. An image of the Alamosa Canyon Bridge test setup is shown in Fig. 10.

A base station was developed for facilitating test operation. This base station served as a communication link with the mobile host, which consisted of a custom-built virtual instrument to acquire, condition, display, and log data transmitted by THINNER and the on- and off-board wireless video cameras (Fig. 11). The software also tracked the voltage across the super capacitor used to power the sensor as well as the RF power transfer efficiency. Additionally, the on/off state and frequency of the RF power transmitter on the mobile host was controlled through this graphical user interface.

A plot showing the charging characteristics of the 0.1 F capacitor connected to the THINNER sensor node with the RF energy transmission from the helicopter is shown in Fig. 12. As can be seen in the plot, it took more than 270 s to reach 3.5 V on the 0.1 F capacitor, which is significantly longer than the laboratory experiment (95 s). The reason for this discrepancy can be attributed to a few factors, including the difficulty of aligning the helicopter with the patch antenna caused by the wind blowing under the bridge. Video footage of the tests shows that the helicopter is constantly traveling in
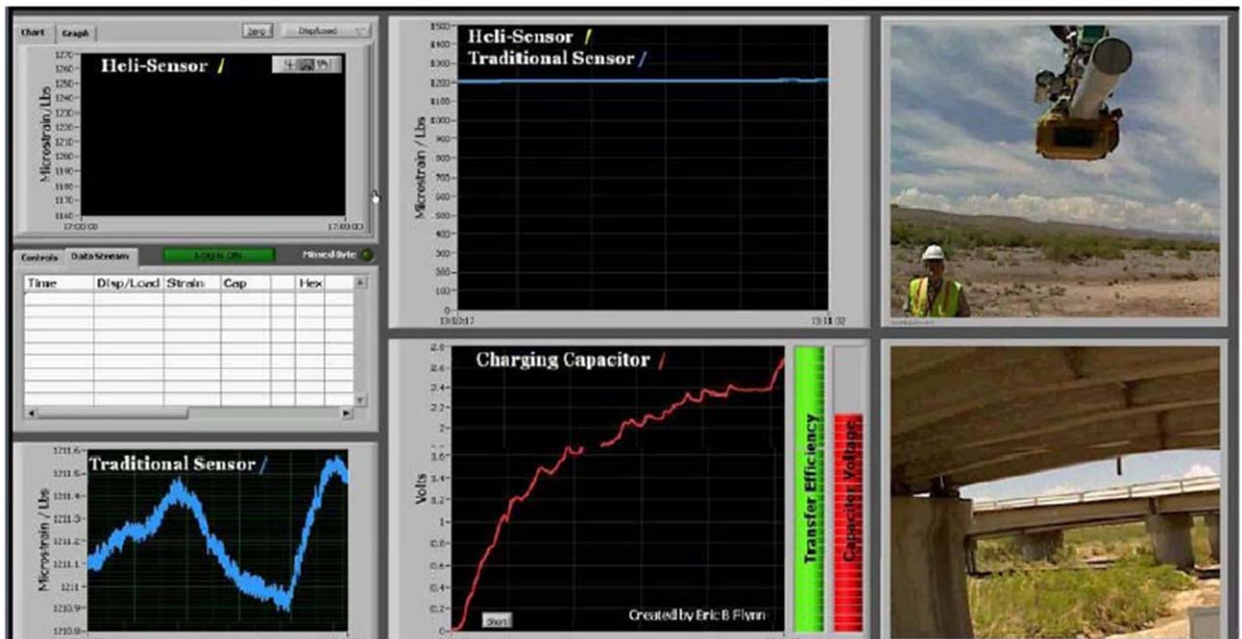

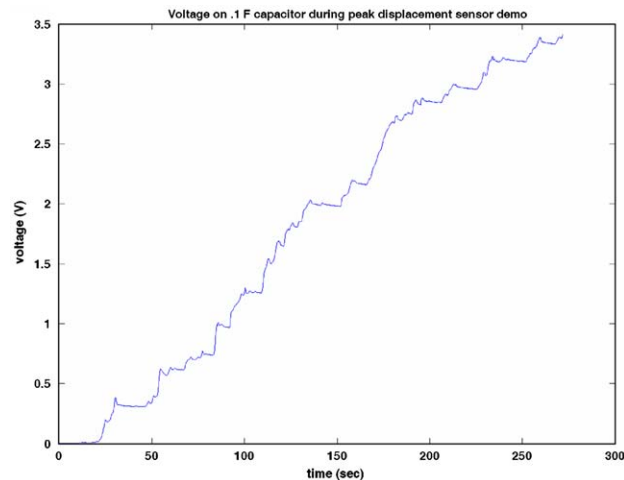Fig. 11. Data acquisition graphical user interface at the base station.

Fig. 12. Voltage on 0.1 F capacitor connected to THINNER as the helicopter charges.

a loop in an effort to maintain the proper distance and orientation of the bridge against the wind. This behavior is also observed in the plot, which exhibits characteristics in common with a stair step. The flat portions of the "stairs" correspond to times when the helicopter was either too far away from the antenna, or was misaligned with the patch antenna. The vertical portions of the "stairs" correspond to the periods where the helicopter was tending to move toward the bridge and/or had the best alignment with the patch antenna. It is estimated that the average power transmission was 2.5 mW, which is significantly lower than the power delivered in the lab. An interesting feature of Fig. 12 is that there is a portion between 166 and 180 s that has a higher power delivery over a characteristically significant time than most of the rest of the plot. Despite the low-power RF energy transmission, the THINNER sensor node was successfully charged to 3.5 V, and the sensor node completed three peak displacement sensor measurements with the energy stored in the 0.1 F capacitor.

Another test was performed after repositioning the patch antenna closer to ground level to improve the accuracy of the alignment between the Yagi antenna on the helicopter and the patch antenna on the bridge, shown in Fig. 13. Mounting the patch antenna close to ground level allowed the pilot a better view for aligning the antennas. Furthermore, aerodynamic forces caused by the wind blowing off the bottom of the bridge were reduced. Once again the helicopter was used to charge up the capacitor connected to the THINNER sensor node. The resulting plot of voltage vs. time is shown in Fig. 14. In this plot, the "stair step" phenomenon is not present to the same degree as in the previous test. The reason the "stair step" effect is gone is due to the fact that the pilot was able to maintain a more constant hover position with the helicopter. The linear fit to the curve in the plot shows that the average power delivered to the capacitor had jumped up to 4.8 mW. Furthermore, the time to charge to 3.5 V was approximately 100 s, which is much closer to the 95 s reported in the lab experiments. These results show that maintaining the proper alignment of the antennas has a very significant impact on

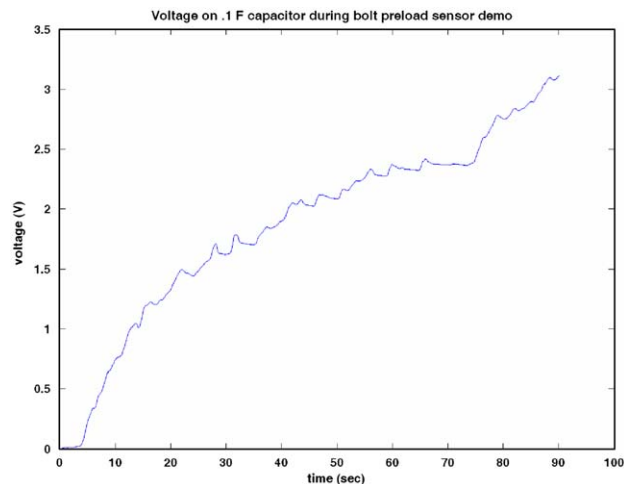**Fig. 13.** THINNER sensor node moved closer to ground level.

Fig. 14. Voltage vs. time for the RF energy transmission test to THINNER mounted close to ground level.

the performance of the RF wireless energy transmission. In this test, four measurements were successfully completed by THINNER. In addition it is also worth noting that the Fig. 14 also shows a period between 75 and 79 s where the power is significantly higher than the other portions of the curve.

5.2. RF energy transmission to the WID2 sensor node using a ground vehicle

The final series of experiments at the Alamosa Canyon Bridge were designed to evaluate the performance while transmitting the energy using a ground vehicle. Because it is much easier to align the antennas using the ground vehicle, it

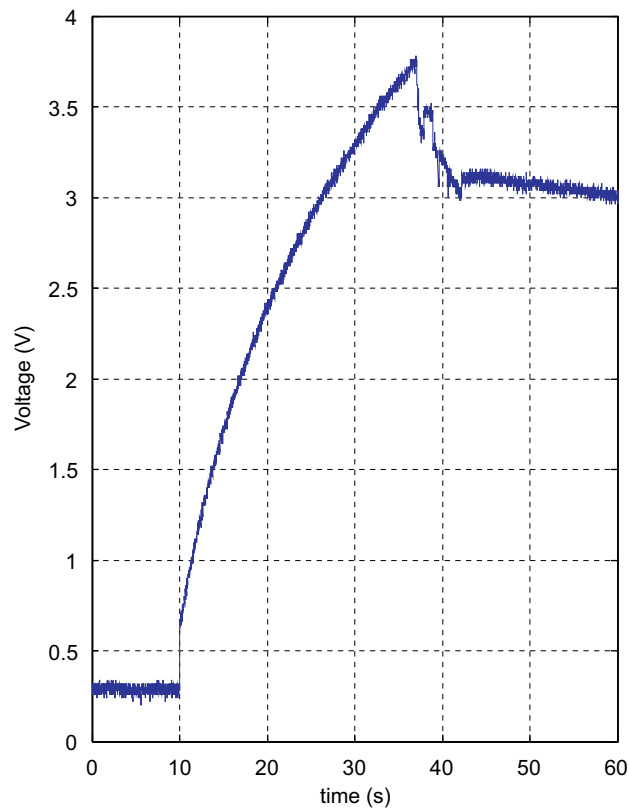**Fig. 15.** Wireless energy transmission system field tested using ground vehicle as a mobile-host.

Fig. 16. Voltage vs. time for the RF energy transmission test to the capacitor connected to WID2.

is expected that the charging time will be much shorter than when using the helicopter. To accomplish this experiment, the WID2 sensor node was mounted along the western rail of the bridge and was connected to three instrumented washers that were mounted using 19 cm steel bolts used to secure a steel cross member to the outer girder of the bridge. The microstrip patch antenna array was mounted near the sensor node as shown in Fig. 15. The WID2 was configured to take measurements and transmit data once powered on by the wireless energy transmission system. A voltage threshold switch described in the previous section was installed, which allowed the capacitor to charge to a predefined voltage of 3.6 V before sending power to the WID2.

The energy transmission equipment was mounted on the mobile host vehicle as shown in Fig. 15. The RF antenna was configured to regulate the output power to 1 W. This system was operated by the driver of the vehicle, and the system was turned off once voltage was supplied to the sensor node. Multiple experiments were performed using this system as the vehicle was driven up to the rectenna, where the vehicle was stopped and energy was beamed to the receiving antenna. Fig. 16 depicts the charging profile within the 0.1 F capacitor as the RF energy was being transmitted. The system was capable of charging the capacitor to a voltage of 3.6 V in an average time of 27 s at a distance of 1.2–1.3 m. In this figure the wireless transmission was initiated at 10 s and approximately 27 s later the power conditioning circuit is triggered, causing the sensor node to become active and take a measurement of the piezoelectric sensors, as indicated by the sharp drop in voltage at 37 s. The voltage then stabilizes as the microcontroller performs local computations between 37.5 and 38.5 s, at which point the sensor node transmits the data to the mobile host as indicated by the voltage drop from 39 to 41 s. There are total 15 bytes of data were transmitted, which is the result of the computation performed by the microcontroller of WID2 regarding the health of the joint.

6. Conclusions

A mobile-host based wireless sensor networking paradigm was proposed and tested for structural health monitoring applications. A commercially available radio-controlled helicopter was equipped to deliver microwave energy to wireless sensor nodes. The helicopter successfully delivered sufficient energy to charge a wireless sensor node that subsequently made multiple peak displacement measurements and transmitted the data back to the helicopter. In addition, the field demonstrations indicate that wireless energy transmission is sufficient for powering the wireless impedance measuring devices, which have previously been developed by the authors for SHM applications. The results of these experiment show that a mobile-host wireless sensor network can feasibly be used to distribute energy to sensor nodes on an as-needed basis and to collect data from these nodes. The advantage of RF energy transmission is that it removes the need to have a conventional limited-life power source embedded within the structure with each sensor node. It should be noted that the proposed approach is only applicable for sensors that do not need to generate a continuous stream of data, such as those based on accelerometers. The integration of the proposed wireless energy transmission with existing energy harvesting techniques to overcome such limitation, i.e., the mobile host augments if energy harvesters do not provide sufficient energy for sensor nodes, is currently being investigated by authors, and is a subject of the next paper.

References

[1] G. Park, C.R. Farrar, M.D. Todd, W. Hodgkiss, T. Rosing, Energy harvesting for structural health monitoring sensor networks, *ASCE Journal of Infrastructure Systems* 14 (2008) 64–79.

[2] C.R. Farrar, G. Park, D.W. Allen, M.D. Todd, Sensor network paradigms for structural health monitoring, *Structural Control and Health Monitoring* 13 (2006) 210–255.

[3] M.D. Todd, D.L. Mascarenas, E.B. Flynn, T. Rosing, B. Lee, D. Musiani, S. Dasgupta, S. Kpotufe, D. Hsu, R. Gupta, G. Park, T. Overly, M. Nothnagel, C.R. Farrar, A different approach to sensor networking for SHM: remote powering and interrogation with unmanned arial vehicles, *Proceedings of Sixth International Workshop on Structural Health Monitoring*, Stanford, CA, September 11–13, 2007.

[4] W.C. Brown, The history of wireless power transmission, *Solar Energy* 56 (1996) 3–21.

[5] G.E. Maryniak, Status of international experimentation in wireless power transmission, *Solar Energy* 56 (1996) 87–91.

[6] S. Choi, K. Song, W. Golembiewskii, S.H. Chu, G. King, Microwave powers for smart material actuators, *Smart Materials and Structures* 13 (2004) 38–48.

[7] D. Pozar, *Microwave Engineering*, third ed., Wiley, 2005, pp. 647–648.

[8] B. Constantine, *Antenna Theory Analysis and Design*, third ed., Wiley, Hoboken, New Jersey, 2005, pp. 50–51 and pp. 66–67.

[9] Cisco Systems Technical Note, Multipath and Diversity, Document ID number 27147, (2006–2007).

[10] Voltage Multipliers Inc. Application Note, *Multipliers—Analysis and Design*, Chapter 13, 1989, pp. 280–294.

[11] A. Mita, S. Takhira, A smart sensor using a mechanical memory for structural health monitoring of a damaged control building, *Smart Materials and Structures* 12 (2003) 204–209.

[12] D.D.L. Mascarenas, E.B. Flynn, M.D. Todd, T.G. Overly, K.M. Farinholt, G. Park, C.R. Farrar, Development of capacitance-based and impedance-based wireless sensors and sensor nodes for structural health monitoring applications, *Journal of Sound and Vibration*, in press, doi:10.1016/j.jsv.2009.07.021.

[13] M. Nothnagel, G. Park, C.R. Farrar, Wireless energy transmission for structural health monitoring embedded sensor nodes, *Proceedings of the SPIE* 6532 (2007) 653216-11.